Accepted Article

Title: Probing the Hydrogen Evolution Reaction and Charge Transfer on Platinum Electrodes on Femtosecond Timescales

Authors: Gregor Zwaschka, Yujin Tong, Martin Wolf, and R. Kramer Campen

This manuscript has been accepted after peer review and appears as an Accepted Article online prior to editing, proofing, and formal publication of the final Version of Record (VoR). This work is currently citable by using the Digital Object Identifier (DOI) given below. The VoR will be published online in Early View as soon as possible and may be different to this Accepted Article as a result of editing. Readers should obtain the VoR from the journal website shown below when it is published to ensure accuracy of information. The authors are responsible for the content of this Accepted Article.

A Journal of

ChemPubSoc
Europe

PROBING THE HYDROGEN EVOLUTION REACTION AND CHARGE TRANSFER ON PLATINUM ELECTRODES ON FEMTOSECOND TIMESCALES

GREGOR ZWASCHKA, DR. YUJIN TONG, PROF. DR. MARTIN WOLF, DR. R. KRAMER CAMPEN[†]

Fritz Haber Institute of the Max Planck Society, Faradayweg 4-6, 14195 Berlin, Germany

ABSTRACT. Despite much study the mechanism of the hydrogen evolution reaction (HER) on Pt is still controversial. Part of the challenge is that any comprehensive description may have to describe processes on timescales from the femtosecond, interfacial electron transfer, to millisecond, ion diffusion. Here we separate these timescales using a femtosecond perturbation approach: we collect cyclic voltammograms from several Pt electrodes with and without femtosecond laser irradiation. We find that at biases near hydrogen evolution laser irradiation lowers the barrier for H_2 generation, while in the H under potential deposition range it induces partial charge transfer along the Pt-H bond and interfacial dipole (re)arrangement. The trend in ultrafast partial charge transfer we measure, Pt(111) < Pt(100) < Pt(110) << Pt microelectrode, is the same as for H_2 generation suggesting insight into both ultrafast electron transfer and slow double layer structural change is required to describe HER mechanism.
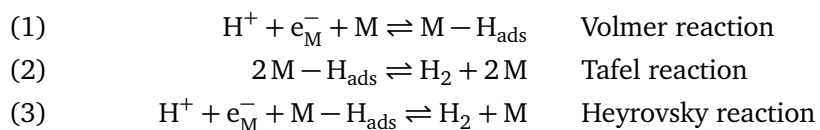
Femtochemistry, Heterogeneous Catalysis, Water Splitting, Photocatalysis, Photochemistry

1. INTRODUCTION

In a prospective hydrogen-based energy economy electrochemical hydrogen conversion in aqueous solutions, *i.e.* the hydrogen evolution and oxidation (HER/HOR) reactions, is expected to play a critical role in energy conversion and storage. Decades of studies clearly demonstrate that while platinum has a unique combination of activity and stability for the HER/HOR in aqueous solution [1, 2], its cost makes large scale deployment of most types of Pt containing devices impractical [3]. Mechanistic understanding of the HER/HOR on Pt, *i.e.* understanding the physics behind Pt's extraordinary combination of activity and stability, should aid in designing new generations of electrocatalysts with superior properties and in creating Pt nanoparticle based materials that preserve the activity and stability of more extended phases at a fraction of the cost [4].

E-mail address: [†]campen@fhi-berlin.mpg.de.

In acidic media, the first step of the HER on Pt is thought to be the reduction of a proton from solution by an electron from the metal leading to a surface Pt-H species: the Volmer reaction (eq. 1, in which e_M^- is a metal electron). In the second step, molecular hydrogen (H_2) is thought to be formed in one of two ways: either by recombinative desorption of two surface Pt-H groups, *i.e.* the Tafel reaction (eq. 2), or by reaction of a surface Pt-H with an aqueous proton and metal electron, *i.e.* the Heyrovsky reaction (eq. 3) [5].

(1) $\qquad\qquad H^+ + e_M^- + M \rightleftharpoons M-H_{ads}$ $\qquad$ Volmer reaction

(2) $\qquad\qquad 2\,M-H_{ads} \rightleftharpoons H_2 + 2\,M$ $\qquad$ Tafel reaction

(3) $\qquad H^+ + e_M^- + M-H_{ads} \rightleftharpoons H_2 + M$ $\qquad$ Heyrovsky reaction

This conceptual model of the HER mechanism on Pt is useful but clearly incomplete: *e.g.* it offers no insight into the relative importance of the Tafel and Heyrovsky reactions for a given electrolyte and Pt electrode [6]. Perhaps more troublingly it cannot rationalize several well established experimental facts: the HER rate changes significantly with changes in Pt surface structure or electrolyte and slows by several orders of magnitude moving from acidic to basic pH [7, 8, 9, 10, 11].

Gaining molecular-level insight into the HER mechanism sufficient to rationalize these experimental observations has proven challenging. Electrochemical studies addressing mechanism, *e.g.* measurement of the Tafel slope, are only indirect [12]. Combinations of these techniques with temperature jump measurements, *ex-situ* measurements or theory have been taken to suggest that the enthalpy of interfacial water hydrogen bonding or the entropy of the interfacial hydronium may explain pH effects [13, 10, 11]. Regardless of the particular conclusions of these and other studies, equations 1 - 3 make clear that a prerequisite to gaining mechanistic insight into the HER on Pt is the ability to characterize surface Pt-H. The great majority of prior electrochemical work has lead to the conclusion that two Pt-H species coexist on the electrode [14, 15, 16, 7, 1]. Under potential deposited hydrogen (H_{UPD}) adsorption starts at 0.4, 0.35 and 0.2 V vs. RHE on Pt(100), Pt(111) and Pt(110), respectively [1], and is argued to be a spectator in the HER [14, 15, 16, 7]. Over potential deposited hydrogen (H_{OPD}) is thought to adsorb near 0 V vs. RHE and to be the HER intermediate [17, 18]. Infrared spectroelectrochemistry studies find a feature assigned to Pt-H that appears at 0.1 V vs. RHE, increases in intensity as potential is scanned negatively, and that, despite the inexact correlation with HER onset in cyclic voltammetry, has been argued to be H_{OPD} [19, 20, 21].

One possible explanation for the evident difficulty in determining the HER/HOR mechanism(s) is that the Volmer, Tafel and Heyrovsky reactions are not true elementary steps in H_2 generation/consumption. For example, in order for the Volmer reaction to happen in acid it seems clear that the excess proton in interfacial water must desolvate, interfacial electrolyte or water must restructure, and an electron must move from the Pt bulk to, at least, a Pt-H surface

state [13]. An experimental approach that would allow us to characterize all of these steps independently would clearly be useful in developing a complete understanding of mechanism. The simplest such experiment one might imagine is the characterization of the structure of the Pt/water interface *operando*, *i.e. during* the HER. However, assuming one could probe all relevant species it is not obvious that such steady-state characterization would offer significant insight into the HER mechanism. Under such conditions we might expect reactant, intermediate and product of the HER, and possible parasitic reactions, to be present in ratios we do not know *a priori*. As a result independent knowledge of reaction mechanism and kinetics would be required to understand the data we hope to use to provide insight into reaction mechanism.

This problem can be circumvented by performing a perturbation experiment: provide a temporally short pulse of reactant(s) and then monitor the time evolution of all interfacial species as the pulse dissipates and the system returns to equilibrium. Because we wish to use the results of this dynamic perturbation approach to gain insight into the mechanism of the HER under potentials relevant to (thermally equilibrated) electrocatalysis, this pulse of reactants should be sufficiently short that it does not perturb double layer structure (*i.e.* lead to ion diffusion within the double layer) and on the natural, femtosecond timescale of electron transfer. Such rapid perturbations are generally not possible using classical electrochemical methods: the response time of an electrochemical cell is > 5 ns for the smallest ultramicroelectrodes and hundreds of microseconds for millimeter-sized, single crystals [22].

Much prior work has shown that chemical reactions can be triggered on metal surfaces on ultrafast timescales using femtosecond laser pulses [23]. The concept is illustrated in Figure 1: an ultrashort laser pulse excites electrons above the Fermi energy (E_F) into a nonthermal distribution of energies. Over the ensuing few hundred femtoseconds these *hot* electrons thermalize to a Fermi-Dirac distribution that, after several picoseconds, equilibrates with the phonon system [24]. From a chemical perspective this transient change in electron energy is equivalent to an ultrafast perturbation of electron chemical potential. These higher chemical potential electrons may, *e.g.* fill Pt-H antibonding states, and induce chemistry that does not occur in their absence.

The possibility of using hot electrons to drive chemistry at extended electrochemical interfaces has been well established in prior studies: Diesing and coworkers have demonstrated that a steady-state supply of *hot* electrons (created employing an electrode that is a metal/insulator/metal junction) catalyzes the HER [25] and Krivenko et al. have shown that subpicosecond laser pulses on Hg or Ag electrodes can drive electrochemistry [26]. In more recent theoretical work, employing a simplified model of electrode electronic structure and reactant, Schmickler and coworkers have found that the effect of hot electrons is to lower the reaction barrier of (both adiabatic and nonadiabatic) electrocatalytic reactions [27].

In this study we collect cyclic voltammograms from a Pt microelectrode and several single crystals in acidic electrolyte in the presence and absence of illumination with 55 femtosecond, 1.56 eV laser pulses. We find that laser irradiation enhances the HER on all surfaces in a manner consistent with hot electron driven chemistry. Curiously, at more positive potentials in the H_{UPD} portion of the cyclic voltammograms, laser irradiation induces a current of opposite sign in the cathodic and anodic scans. A series of control experiments demonstrate that at these more positive potentials the effect of laser irradiation is to induce partial charge transfer on sub-picosecond timescales the extent of which is a function of Pt surface and interfacial electrolyte structure. The charge transfer dynamics we observe are sufficiently fast that, in contrast to conventional measurements of electrochemical charge transfer resistance, they are the result solely of the elementary step of transferring an electron from the Pt electrode to the adsorbate and are relatively uninfluenced by the, slower, dynamics of proton desolvation or ion diffusion within the electrolyte. Additionally these observations demonstrate the possibility of initiating charge transfer and the HER on Pt with femtosecond precision: a prerequisite to full experimental insight into the mechanism of this important chemistry.
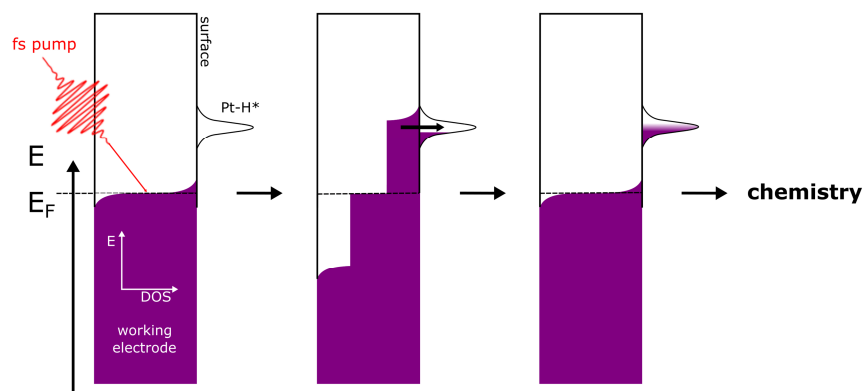

FIGURE 1. Schematic representation of the density of states (DOS) of the working electrode at a fixed potential that is set by the potentiostat before arrival of the laser pulse (left), before electron thermalization (middle) and after electron thermalization (right). In this scheme the excitation leads to population of a Pt-H anti-bonding state.

2. RESULTS AND DISCUSSION

The lower panel of Figure 2 shows cyclic voltammograms (CVs) of a Pt microelectrode collected in a thin film spectroelectrochemical cell in the presence and absence of pulsed – *i.e.* 1.56 eV, 55 fs, 1 KHz repetition rate – laser irradiation. As we show in Figure S1 in the Supporting Information, after an induction period the laser-induced changes in the CV are stable over many voltammetric cycles

and are reversible. While the electrode's size precludes detailed structural characterization, its CV shows clear current features at $\approx$ 0.3 and 0.1 V vs. RHE, consistent with H_{UPD} adsorption on the Pt(100) and (110) surfaces respectively. In agreement with much prior work, anodic H_{UPD} current features are somewhat larger than cathodic presumably because of a minor oxygen impurity in the electrolyte and the resulting contribution of the oxygen reduction reaction to our voltammogram [28].

The features of the CV are affected by illumination as follows. Firstly, as shown in the inset, and as predicted for a reaction driven by hot electrons, the HER current is increased and shifted to more positive potentials with higher laser fluences leading to larger shifts in potential. Secondly, H_{UPD} related currents, *i.e.* between 0.35 and 0 V, are decreased to a varying extent as a function of potential in both the cathodic and anodic scans[a]. As highlighted in the I_{illum}/I_{dark} ratio in the upper panel of Figure 2, the effect of laser illumination on H_{UPD} current reaches a maximum at potentials of maximum H_{UPD} current in the absence of illumination at all fluences (see insets to Figure 2 for fluence dependent laser-induced current). Apparently, despite the 1.56 eV photon energy of laser illumination far exceeding the 1.23 V window of water's thermodynamic stability, laser-induced currents are strongly modulated by mV changes in the working electrode bias. While such small changes in bias are relatively unimportant from the perspective of the electronic structure of Pt, much prior work suggests that they can drastically alter the structure of interfacial electrolyte [29, 30]: evidently the amplitude of the laser-induced H_{UPD} current depends on interfacial electrolyte structure.

While it is clear from the data that we measure a laser-induced current at the Pt electrode, the origin of this current, and its relationship to *hot* electrons, is not. We imagine five possible causes of the laser-induced current: (i) chemistry that is initiated by heating of the interfacial region; (ii) direct optically resonant charge transfer from the metal to an adsorbate electronic state; (iii) solution phase photochemistry; (iv) hot electron driven chemistry; or (v) laser-induced changes in interfacial polarization, either by charge transfer along the Pt-H bond or a laser-induced rearrangement of interfacial structure [31].

Each of these possible origins of the laser-induced current depends differently on the properties of the laser illumination and Pt surface structure. The results of experiments exploring the dependence of the laser-induced current on fluence are shown in Figure 2 and Figure 3a and those describing the dependence of the laser-induced current on pulse length and photon energy in Figure 3b. To evaluate the effect of Pt surface structure on our measured observables we also collect cyclic voltammograms under 55 femtosecond illumination for a variety of

---

[a]The H_{UPD}(110) feature, *i.e.* the current feature at 0.1 V, is enhanced by laser illumination in the cathodic scan but suppressed in the anodic: the laser induced current is the same sign in both scan directions. This relationship does not hold for the Pt(100) H_{UPD} feature on the microelectrode or on the single crystal CVs. This trend is consistent with the reduction of trace O_2 concentrations in our thin-film spectroelectrochemical cell. See Supporting Information for more detailed discussion.
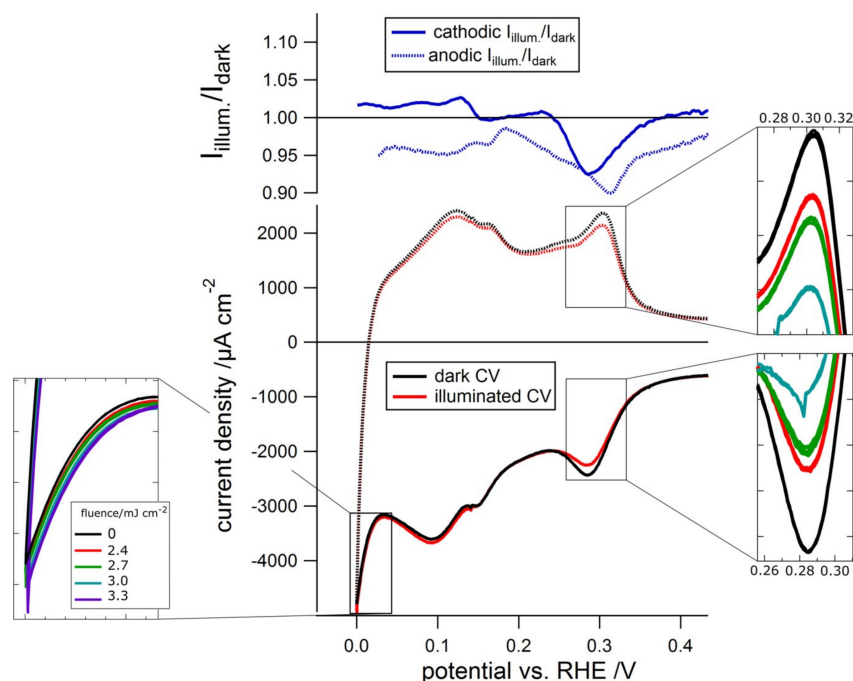
FIGURE 2. The lower panel shows CVs of a Pt microelectrode electrode with a film thickness in our spectroelectrochemical of 5 μm at 500 mV/s with (red) and without (black) femtosecond near-IR irradiation in 0.05 M H$_2$SO$_4$. For the illumination, 2.4 mJ/cm$^2 \cdot$pulse of 800 nm, 55 fs radiation (1 kHz repetition rate) was used. The upper panel shows the ratio of the illuminated over not illuminated CVs as blue traces, solid (dotted) lines are cathodic (anodic) scans. On the left excerpts of the HER region and right H$_{UPD}$ sorption on the (100) site each with varying laser fluence (given in the legend of the HER inset) are shown.

single crystal surfaces (see Figure 4 for data and below for detailed discussion). For comparison of laser-induced current under these different conditions it is convenient to extract two metrics: a measure of the effect of laser illumination on the HER and on H$_{UPD}$. For the former we take the currents at 0 V vs. RHE in the presence and absence of illumination and calculate $[(^{(I_{illum}-I_{dark})}/I_{dark}) \times 100]$. For the latter we extract the laser-induced, *i.e.* $[(^{(I_{illum}-I_{dark})}/I_{dark}) \times 100]$, H$_{UPD}$ current. Because the bias at which H$_{UPD}$ current features appear is surface structure dependent we compare current ratios at different potentials on different surfaces. The details of this choice of metric, the demonstration that our results are qualitatively insensitive to this choice and to the presence of defects on the single crystal surfaces, are shown in the Supporting Information.

If our laser-induced current was the result of solution heating – either because of heat induced reactions in bulk electrolyte or because of increased H$_2$
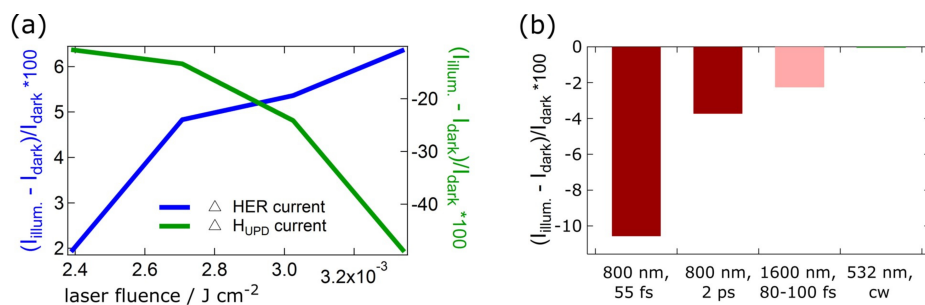
FIGURE 3. (a) The change of the $\left[\frac{I_{illum}-I_{dark}}{I_{dark}} \times 100\right]$ ratio at 0.3 V vs. RHE in the anodic scan of the CV shown in Figure 2 (green trace, H_{UPD}) and at 0 V vs. RHE (blue trace, HER) with linearly increasing laser fluence. (b) The $\left[\frac{I_{illum}-I_{dark}}{I_{dark}} \times 100\right]$ ratio at 0.3 V in the anodic scan of four different experiments in which the microelectrode was illuminated with the same laser fluence (2.4 $\mathrm{mJ/cm^2 \cdot pulse}$), but different wavelengths and pulse durations. Experimental details are the same as is in Figure 2.

interfacial diffusivity – the laser-induced current should (a) be insensitive to pulse length, (b) given simple Arrhenius kinetics for the HER (in which the prefactor is temperature independent) increase exponentially with a linear increase in incident pulse energy (*i.e.* a linear increase in temperature) and (c) be insensitive to changes in surface structure. The signal we observe clearly varies strongly with pulse length (Figure 3b) , changes nonexponentially with changes in laser fluence (Figure 3a) and changes strongly with surface structure (Figure 4). We therefore conclude our results cannot be explained by solution heating. If the laser-induced currents were the result of 1 photon resonant excitation of electrons into an adsorbate surface state the measured current should be independent of pulse duration. As shown in Figure 3b this is clearly not the case. Similarly, if our measured laser-induced currents could be explained by solution phase photochemistry we would expect them to be independent of surface structure. Clearly, as shown in Figure 4, this is not the case.

We thus conclude that the laser-induced currents are the result of a hot electron driven process. However, because the HER at 0 V and the H_{UPD} at 0.3 V vs. RHE are affected differently by the illumination (as displayed in the insets of Figure 2 and Figures 3a), the microscopic mechanism must differ. As we show in Figure 2 and 3 (and in the Supporting Information for single crystal Pt electrodes) laser illumination shifts the the onset of HER to more positive potentials. This change is consistent with a scenario in which the barrier for the HER has been lowered, either through transfer of population to Pt-H antibonding states or vibrational excitation of the Pt-H bond. This scenario is also consistent with prior experimental [26, 25] and theoretical work [32, 27] where the prior

experimental studies utilized different ways of generating hot electrons and theoretical treatments employ relatively simplified models.

Understanding the origin of the laser-induced H_{UPD} current is more challenging. As shown clearly in Figure 2 for the microelectrode and in the Supporting Information for the single crystal surfaces, the sign of the laser-induced current changes with scan direction: in *both* the cathodic *and* anodic scans laser illumination either decreases, in the case of the microelectrode, or increases, in the case of the single crystal surfaces, the measured current relative to a CV collected in the dark. If, for example, the laser-induced H_{UPD} current on the microelectrode were to be the result of laser-induced redox chemistry (*e.g.* change in population of Pt-H) it would imply that in the cathodic scan laser illumination leads to oxidation of Pt-H and in the anodic scan to reduction. Because there is no physical mechanism that could accomplish this effect, we assign the laser-induced H_{UPD} current to a redistribution of charge *without* a change in population of Pt-H. To develop a qualitative understanding of such effects it is useful to briefly remind ourselves of the fate of ionic charge on adsorption to a metal electrode.

An ion of valence z that strongly adsorbs on a metal electrode surface discharges. Because the electroneutrality of the solution must be maintained, the resulting current flows along the external circuit of the potentiostat and is discharged to the electrolyte at the counter electrode. Actually measuring the current resulting from ion discharge is not generally possible for two reasons: most often discharge is fractional and during discharging both the adsorbate and interfacial solvent/electrolyte dipoles will rearrange to compensate. The former characteristic means it is difficult to understand whether a small measured current implies a fractional discharge of a high density adsorbate or a full discharge of a lower, while rearrangement of interfacial dipoles also contributes to the measured current through causing changes in interfacial capacitance. The combined current that results from ion discharge on adsorption (*id*) and interfacial dipole rearrangement (*dr*) is termed the electrosorption valency (ESV). While the possibility of defining ESV in a model-free, thermodynamically exact manner is controversial [33, 34], for our purposes we wish only to ask whether qualitative insight is possible into the manner in which laser illumination might effect ion discharge and dipole rearrangement. With this goal in mind we write the laser-induced ESV (*l*) for a system with constant surface excess as [31]:

$$(4) \qquad l = \frac{1}{F}\left(\frac{\partial \mu_{(Pt-)H}}{\partial E}\right)_{\Gamma_S} \;=\; id + dr$$

$$id \;=\; z\boldsymbol{g} - \lambda(1 - \boldsymbol{g})$$

$$dr \;=\; \frac{m_{(Pt-)H/W/Elec}}{ed'}$$

where F is Faraday's constant, $\Gamma_{(Pt-)H}$ the surface excess of adsorbed H, $\mu_{(Pt-)H}$ the chemical potential of adsorbed H and E the bias. z is the valence of the adsorbing ion. $\boldsymbol{g}$, the "thickness ratio", is defined $\boldsymbol{g} = \frac{E_{ad} - E_{el}}{E_m - E_{el}}$ where E_{ad} is the potential at the adsorbate, E_{el} the potential at the electrolyte and E_m the potential

of the metal electrons. In the case of completely discharged adsorbates, *e.g.* UPD layers, g is typically taken to be equal to 1 and implies the distance between the surface and inner Helmholtz plane is small relative to that between the inner and outer Helmholtz planes [35]. λ is the partial charge transfer coefficient (and is negative one for a fully discharged monovalent cation). $m_{(Pt-)H/W/Elec}$ is the sum of the projection of the Pt-H dipole, the dipoles of interfacial water and electrolyte dipoles on the surface normal, d' is the double layer thickness divided by the interfacial dielectric constant and e the elemental charge. The derivation of Eq. 4 and a more detailed description of the parameters can be found in a recent review by Schmickler and coworkers [31].

The 1.56 eV photon energy of our excitation is well in excess of that necessary to excite Pt electrons into Pt-H anti-bonding states [36]. Such an excitation energy is expected to decrease the value of g (it would change the metal electron potential but not alter the potential at the adsorbate or within the electrolyte) and decrease $|\lambda|$ (population of Pt-H anti-bonding states *reduces* net charge transfer to Pt). Thus we expect laser illumination to *decrease* the id term. Clearly changing the extent of ion discharge may lead to a change in structure of either the adsorbate, interfacial water molecules or interfacial electrolyte. Because we have no independent knowledge of interfacial structure we conclude that the *dr* contribution to the laser-induced current may be *either positive* or *negative*. The results for the Pt microelectrode in Figure 2 clearly show laser illumination *decreases* H_{UPD} current. The sign of this effect is thus consistent with a mechanism in which the laser-induced current is the result of both partial charge transfer along the Pt-H bond and, possibly, interfacial structure rearrangements that either lead to a decrease in *dr* or an increase in *dr* less than the decrease in *id*.

Our Pt microelectrode results thus clearly suggest that we induce the HER (near 0 V vs. RHE) and charge transfer (at 0.3 V vs. RHE) with femtosecond laser illumination; and that the size of the laser-induced currents are bias dependent. While changing bias changes interfacial solvent and electrolyte structure [29, 30], *interphase* structure may also be changed by changing the arrangement of surface Pt atoms. As mentioned above, while our Pt microelectrode has H_{UPD} current features similar those on Pt(100) and (110) surfaces in the cyclic voltammogram, the size of these crystallites and the relationship of these structural characteristics to interfacial water or Pt-H orientation are difficult to discern. To better understand these effects we conducted the same type of measurements on Pt single crystals.

The $[(I_{illum}-I_{dark}/I_{dark}) \times 100]$ ratios for the single crystal and microelectrode HER are plotted in the upper panel and those for the H_{UPD} current features in the lower panel of Figure 4. Clearly, on all surfaces laser illumination acts to enhance the HER current. As for the microelectrode, laser-induced H_{UPD} related currents change sign with the scan direction (see Supporting Information for additional data). Similarly we thus conclude that the laser-induced H_{UPD} current on the single crystals cannot be explained by a change in interfacial Pt-H population: it is the result either of charge redistribution along the Pt-H bond or interfacial dipole rearrangement. In contrast to the laser-induced microelectrode

H_{UPD} current, however, on the single crystals laser illumination acts to *increase* the H_{UPD} feature in both scan directions.

Because laser-induced changes in *id* are expected to be only negative, this suggests the laser-induced H_{UPD} currents on the single crystals are dominated by changes in structure of interfacial solvent or adsorbate: changes in interfacial structure overcompensate changes in charge density along the Pt-H bond. Prior experiment and theory have found that extended, long-lived hydrogen bonding structures may develop in interfacial water at Pt single crystals but not at more disordered metal surfaces. Perturbation of this structured interfacial water is expected both to have a larger energetic cost than that for more disordered interfacial water and, because it involves the concerted breaking and reformation of many hydrogen bonds, to happen on picosecond and longer timescales [37, 11]. Interestingly, while the Pt microelectrode shows Pt(100) and (110) H_{UPD} current features in the CV, the effect of laser illumination on these features on the microelectrode and Pt(100) and (110) single crystals is quite different. This comparison, presumably, suggests solvent structures on the single crystals are more extensive than the (micro)crystallites of Pt(100) or (110) necessary to generate current features in the microelectrode CV. It is worth noting that, as discussed in the Supporting Information in detail, our single crystal surfaces are not defect free. Nevertheless this qualitative change in the sign of the laser-induced current relative to the microelectrode suggests that defect densities must be substantially lower than the microelectrode and, presumably sufficiently low that they do not perturb crystal-face dependent electrolyte structure.

Our H_{UPD} observable can be understood as a measure of ease of charge transfer on femtosecond time scales. As we demonstrate above this ease of charge transfer is a function both of Pt surface structure, *i.e.* it varies between the single crystals and the microelectrode, and interfacial electrolyte structure, *i.e.* it varies with bias. A related quantity, the so-called electrochemical charge transfer resistance (ECTR), can be measured using standard potentiostats. This ECTR differs from our observable in that it integrates over electrolyte and solvent restructuring dynamics much slower than the subpicosecond dynamics we observe. Interestingly, however, trends in measured ECTR are similar to those in laser-induced H_{UPD}. Polycrystalline Pt has a measured ECTR of 0.05 $\Omega \cdot cm^2$ [38] while Pt(111) is 0.03 $\Omega \cdot cm^2$ [39] (both in 0.1 M $HClO_4$). Similarly Durst et al. have recently reported the bias dependent ECTR for H_{UPD} adsorption on (110) sites on polycrystalline Pt in alkaline electrolyte. Consistent with our measurements in acid they find the ECTR reaches a minimum, *i.e.* charge transfer is most favorable, at the H_{UPD} current maximum [9]. The coincidence of our measured laser-induced H_{UPD} currents and these earlier ECTR studies suggests that the ease of charge transfer across the Pt/aqueous electrolyte interface is a function of interface structure, both from the Pt and electrolyte side, but independent of slower electrolyte reorganization (*e.g.* ion rotation or translation) dynamics.

Our results thus suggest that partial charge transfer along the Pt-H bond is a function of both Pt surface and interfacial electrolyte structure and that the ease
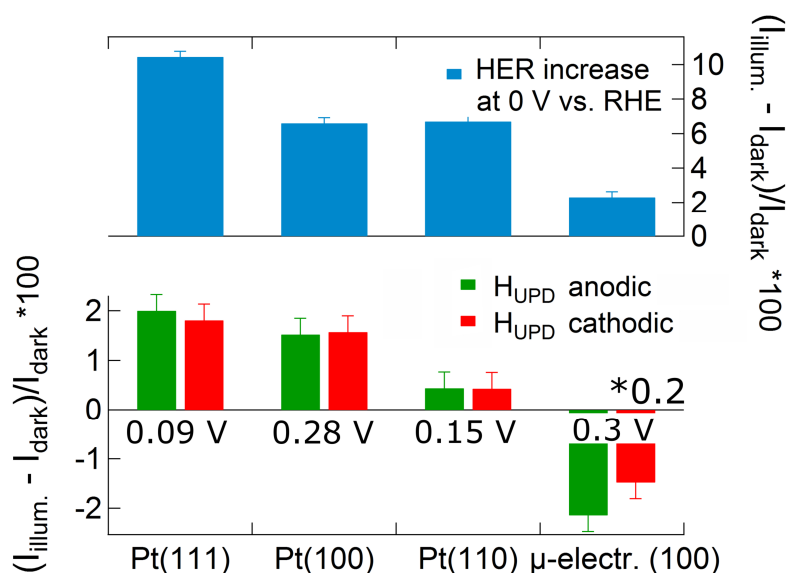
FIGURE 4. Results for four different electrode surfaces, displayed as the $\left[\frac{I_{illum} - I_{dark}}{I_{dark}} \times 100\right]$ ratios at the indicated potentials. 0.5 M H_2SO_4 was used as electrolyte for the single crystal experiments, while 0.05 M H_2SO_4 was used for the microelectrode. 1.8 mJ/cm²·pulse of 800 nm, 55 fs radiation (1 kHz repetition rate) was used for all single crystal experiments, while the microelectrode experiment was conducted with 2.4 mJ/cm²·pulse. The upper panel shows the change in HER current at 0 V vs. RHE upon illumination, and the lower changes in laser-induced H_{UPD} current in both scanning directions. Uncertainty estimate is from replicated measurements.

of such charge transfer increases Pt(111) < Pt(100) < Pt(110) < microelectrode. Prior work measuring HER activity on Pt in acidic media suggests a trend with structure that is the same Pt(111)<Pt(100)<Pt(110)<Pt clusters [7, 40]. Taken together these results suggest that the elementary step of electron transfer, given reactants and a solvation shell in the optimal configuration set by bias, is rate limiting for the HER on Pt in acid.

3. SUMMARY & CONCLUSIONS

In this study we record cyclic voltammograms from a variety of Pt working electrodes in acid in the presence and absence of illumination by 1.56 eV, femtosecond laser pulses. We show that the laser-induced currents we observe decrease dramatically as pulse lengths are extended to > picoseconds and photon energy is decreased, and are a function of Pt surface. These data are most

simply understood if laser irradiation generates a population of hot electrons that at potentials of H_{UPD} deposition cause partial charge transfer along the Pt-H bond, and at those of hydrogen evolution lower the barrier for the reaction. Importantly, despite the photon energy being larger than the 1.23 V water window and thus in principle capable of initiating charge transfer at any bias, significant laser-induced currents appear only at potentials at which H adsorption or HER features appear in the absence of laser illumination. This result implies that the ultrafast current flow we detect requires a "prearranged" double layer structure that is determined by potential. Whatever the details of the double layer structure are that allow electron transfer, these results make clear that they must undergo structural fluctuations on timescales greater than three picoseconds.

We find that ease of electron transfer along the Pt-H bond on ultrafast timescales at H_{UPD} potentials increases in the order Pt(111) < Pt(100) < Pt(110) < Pt microelectrode, the same as that of trends in Pt HER activity in acid measured by prior workers. This correlation (and the bias dependence of the laser-induced current) is consistent with a scenario in which, once interfacial electrolyte and water are in the optimal configuration (as set by the external bias) the ease of charge transfer along the Pt-H bond determines reactivity. Put another way, given a prearranged, optimal interfacial electrolyte structure set by the external bias, HER activity is determined by electron transfer kinetics. Current work in our group focusses on direct characterization of interfacial water and electrolyte structure following femtosecond excitation, within the H_{UPD} and hydrogen evolution potential regions, using time-resolved, nonlinear optical probing of the electrode/electrolyte interface with the goal of determining what, exactly, such an *optimal* configuration might entail.

More generally it is worth noting that virtually all (photo)electrocatalytic systems are composed of elementary steps whose timescales range from the few femtosecond, *e.g.* electron dynamics in metals, to milliseconds, *e.g.* diffusion of counterions through the double layer. Quantitative understanding of reaction mechanisms in (photo)electrocatalysis requires understanding how these processes at widely different timescales interact. While the independent characterization of processes operating at such disparate timescales is not possible in most conventional electrochemical characterization, the approach we describe in this study, in which the chemistry of interest is triggered at a well-defined, on femtoseconds, time and evolution of the interface characterized with femtosecond resolution thereafter, overcomes this hurdle. We thus expect that our approach, and its combination with other probing techniques, will have a large role to play in understanding mechanism in (photo)electrocatalysis in the future.

4. EXPERIMENTAL

The measurements were conducted in a homebuilt, all glass, thin-film spectroelectrochemical cell that allows for purging with inert gas during the measurement and illumination of the electrode surface with laser light. A sketch of

the cell can be found in Figure S7 in the Supporting Information. The glassware was cleaned by (1) immersion in alkaline permanganate solution for 24 h (2) immersion in Piranha solution for 2 h and (3) repeated supersonication in ultrapure water. Exact details of the cleaning procedure for the glassware can be found in our previous work [41]. All solutions were prepared from Milli-Q water and Suprapur sulfuric acid (Merck). The single crystalline working electrodes (5 mm diameter, 3 mm thick, MaTeck) were flame annealed in a butane air flame (for 4 x 1 min plus 1 x 15 min), cooled in water saturated N_2, and then quenched in and covered with a droplet of N_2 purged Milli-Q water. Electrolyte and quenching water were deaerated with gaseous N_2 evaporated off of the liquid. After the active area of the working electrode was covered with a droplet of Milli-Q water its sides were wrapped in Teflon, rinsed thoroughly with Milli-Q water, and then the electrode was transferred to the cell. A homebuilt reversible hydrogen electrode was used as a reference [42].

Because we eventually wish to characterize the Pt/electrolyte interface after laser induced chemistry optically, we performed all single crystal measurements with 1-2 micron thickness of electrolyte above the electrode. At these distances we found it quite challenging to measure the CVs characteristic of the defect-free Pt(111), Pt(110) and Pt(100) surfaces within the cell. While much of our current work explores differently designed sample cells that will, hopefully, avoid this limitation, the presence of *defect-like* features does offer us the possibility of extracting the laser-induced H_{UPD} current from the different single crystals in different ways. This comparison – see Supporting Information for details – suggests that the laser-induced effects we observe on the single crystals are not sensitive to moderate defect densities. The Pt microelectrode (MPTE Micro Platinum electrode 100 micrometer diameter, GAMEC Analysentechnik) was prepared by polishing with a diamond and then with alumina paste. Subsequently, it was cleaned by rinsing with Milli-Q water and placing it in a beaker with Milli-Q water for three cycles in supersonic bath (with fresh Milli-Q water for every round).

We employed a laser system consisting of a Ti:Sapphire oscillator (Vitesse, Coherent), a regenerative 1 kHz amplifier (Legend Elite Duo, Coherent) and an optical parametric amplifier (TOPAS-Prime, Light Conversion) for the generation of the 800 and 1600 nm subpicosecond pulses. The 800 nm picosecond pulses were generated by directing the 800 nm, 55 fs pulses through an air spaced Etalon (SLS Optics Ltd.). The light was propagated to the surface at an angle of 45° and focused using a 1000 mm N-BK7 lens.

SUPPORTING INFORMATION

Data showing stability of the laser-induced current, a detailed justification for the choice of metric used to compare the laser induced chemistry on different electrodes (including the CVs of the single crystal electrodes with and without illumination), discussion of the influence of dissolved O_2 on the microelectrode CV, and details of the spectroelectrochemical cell.

REFERENCES

[1] N. M. Marković, P. N. Ross, *Surf. Sci. Rep.* **2002**, *45*, 117–229.

[2] P. C. K. Vesborg, B. Seger, I. Chorkendorff, *J. Phys. Chem. Lett.* **2015**, *6*, 951–957.

[3] H. A. Gasteiger, S. S. Kocha, B. Sompalli, F. T. Wagner, *Appl. Catal. B* **2005**, *56*, 9–35.

[4] E. Kemppainen, A. Bodin, B. Sebok, T. Pedersen, B. Seger, B. Mei, D. Bae, P. C. K. Vesborg, J. Halme, O. Hansen, P. D. Lund, I. Chorkendorff, *Energy Environ. Sci.* **2015**, *8*, 2991–2999.

[5] K. Krischer, E. R. Savinova in *Handbook of Heterogeneous Catalysis* (Eds.: G. Ertl, H. Knözinger, F. Schüth, J. Weitkamp), Wiley-VCH Verlag GmbH & Co, **2009**, Chapter 8.1. Electrocatalysis, pp. 1873–1905.

[6] S. Watzele, J. Fichtner, B. Garlyyev, J. N. Schwämmlein, A. S. Bandarenka, *ACS Catal.* **2018**.

[7] N. M. Marković, B. N. Grgur, P. N. Ross, *J. Phys. Chem. B* **1997**, *101*, 5405–5413.

[8] R. Subbaraman, D. Tripkovic, K.-C. Chang, D. Strmcnik, A. P. Paulikas, P. Hirunsit, M. Chan, J. Greeley, V. Stamenkovic, N. M. Markovic, *Nat. Mater.* **2012**, *11*, 550.

[9] J. Durst, A. Siebel, C. Simon, F. Hasche, J. Herranz, H. Gasteiger, *Energy Environ. Sci.* **2014**, *7*, 2255–2260.

[10] J. Rossmeisl, K. Chan, E. Skúlason, M. E. Björketun, V. Tripkovic, *Catal. Today* **2016**, *262*, 36–40.

[11] I. Ledezma-Yanez, W. D. Z. Wallace, P. Sebastián-Pascual, V. Climent, J. M. Feliu, M. T. Koper, *Nat. Energy* **2017**, *2*, 17031.

[12] T. Shinagawa, A. T. Garcia-Esparza, K. Takanabe, *Sci. Rep.* **2015**, *5*, 13801.

[13] A. R. Zeradjanin, A. Vimalanandan, G. Polymeros, A. A. Topalov, K. J. Mayrhofer, M. Rohwerder, *Phys. Chem. Chem. Phys.* **2017**, *19*, 17019–17027.

[14] E. Protopopoff, P. Marcus, *J. Vac. Sci. Technol. A* **1987**, *5*, 944–947.

[15] E. Protopopoff, P. Marcus, *J. Chim. Phys. Phys.-Chim. Biol.* **1991**, *88*, 1423–1452.

[16] N. M. Marković, S. T. Sarraf, H. A. Gasteiger, P. N. Ross, *J. Chem. Soc. Faraday Trans.* **1996**, *92*, 3719–3725.

[17] B. E. Conway, L. Bai, *J. Chem. Soc. Faraday Trans. 1* **1985**, *81*, 1841–1862.

[18] B. E. Conway, *Sci. Prog. (1933-)* **1987**, 479–509.

[19] R. J. Nichols, A. Bewick, *J. Electroanal. Chem. Interfacial Electrochem.* **1988**, *243*, 445–453.

[20] K. Kunimatsu, T. Senzaki, G. Samjeské, M. Tsushima, M. Osawa, *Electrochim. Acta* **2007**, *52*, 5715–5724.

[21] M. Nakamura, T. Kobayashi, N. Hoshi, *Surf. Sci.* **2011**, *605*, 1462–1465.

[22] C. G. Zoski, *Handbook of Electrochemistry*, Elsevier, **2007**.

[23] C. Frischkorn, M. Wolf, *Chem. Rev. (Washington DC U. S.)* **2006**, *106*, 4207–4233.

[24] E. Knoesel, A. Hotzel, M. Wolf, *Phys. Rev. B* **1998**, *57*, 12812.

[25] D. Diesing, G. Kritzler, M. Stermann, D. Nolting, A. Otto, *J. Solid State Electrochem.* **2003**, *7*, 389–415.

[26] A. Krivenko, J. Krüger, W. Kautek, V. Benderskii, *Ber. Bunsenges. Phys. Chem.* **1995**, *99*, 1489–1494.

[27] R. R. Nazmutdinov, I. R. Manyurov, W. Schmickler, *Chem. Phys. Lett.* **2006**, *429*, 457–463.

[28] N. M. Markovic, H. A. Gasteiger, P. N. Ross Jr, *J. Phys. Chem.* **1995**, *99*, 3411–3415.

[29] K.-i. Ataka, T. Yotsuyanagi, M. Osawa, *J. Phys. Chem.* **1996**, *100*, 10664–10672.

[30] Y. Tong, F. Lapointe, M. Thämer, M. Wolf, R. K. Campen, *Angew. Chem. Int. Ed.* **2017**, *56*, 4211–4214.

[31] W. Schmickler, R. Guidelli, *Electrochim. Acta* **2014**, *127*, 489–505.

[32] J. W. Gadzuk, *Chem. Phys.* **2000**, *251*, 87–97.

[33] V. A. Marichev, *Surf. Sci. Rep.* **2005**, *56*, 277–324.

[34] B. B. Damaskin, O. A. Petrii, *J. Solid State Electrochem.* **2011**, *15*, 1317–1334.

[35] J. Schultze, D. Rolle, *Can. J. Chem.* **1997**, *75*, 1750–1758.

[36] B. Hammer, J. Norskov, *Nature* **1995**, *376*, 238.

[37] D. T. Limmer, A. P. Willard, P. Madden, D. Chandler, *Proc. Natl. Acad. Sci. U. S. A.* **2013**, *110*, 4200–4205.

[38] B. Łosiewicz, R. Jurczakowski, A. Lasia, *Electrochim. Acta* **2012**, *80*, 292–301.

[39] E. Sibert, R. Faure, R. Durand, *J. Electroanal. Chem.* **2001**, *515*, 71–81.

[40] A. R. Kucernak, C. Zalitis, *J. Phys. Chem. C* **2016**, *120*, 10721–10745.

[41] G. Zwaschka, M. Wolf, R. K. Campen, Y. Tong, *Surf. Sci.* **2018**, *678*, 78–85.

[42] P.-O. Eggen, *J. Chem. Educ.* **2009**, *86*, 352.
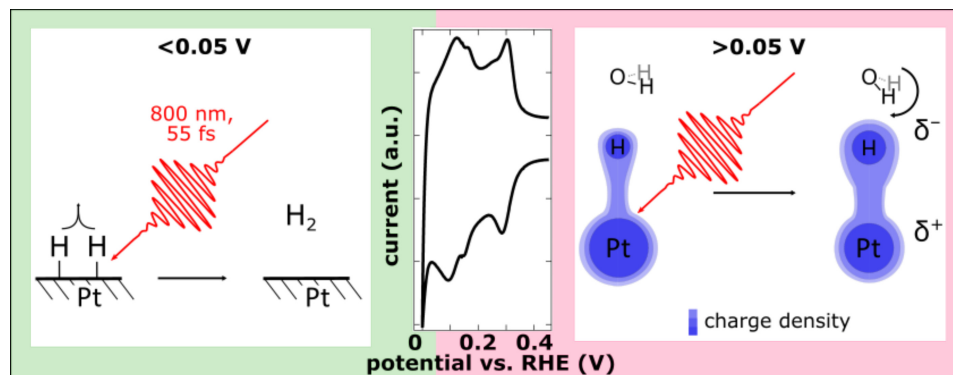
TABLE OF CONTENTS GRAPHIC

TABLE OF CONTENTS TEXT

We study the hydrogen evolution reaction (HER) on Pt via photocurrents induced by femtosecond illumination. The relative ultrafast partial charge transfer between Pt surfaces correlates with H_2 generation suggesting HER elementary steps include ultrafast e^- transfer and slow double layer change.